I. Manika, R. Zabels, J. Maniks, K. Schwartz, R. Grants, T. Krasta, A. Kuzmin,
Formation of dislocations in LiF irradiated with 3He and 4He ions,
J. Nucl. Mater. 507 (2018) 241-247.

FORMATION OF EXTENDED DEFECTS IN LiF IRRADIATED WITH ^{3}He AND ^{4}He IONS

I. Manika[1], R.Zabels[1], J.Maniks[1], K.Schwartz[2], R. Grants[1], T.Krasta[1], A.Kuzmins[1]

[1]Institute of Solid State Physics, University of Latvia, 8 Kengaraga str., LV-1063 Riga, Latvia

[2]GSI Helmholtzzentrum für Schwerionenforschung, 1 Planckstr., 64291 Darmstadt, Germany

ABSTRACT

Influence of the irradiation with 13.5 MeV ^{3}He and 5MeV ^{4}He ions on the micro-structure and mechanical properties of LiF single crystals was studied. The depth profiles of nanoindentation, dislocation mobility, selective chemical etching and photoluminescence served for the characterization of damage. Strong ion-induced increase of hardness and decrease in dislocation mobility at the stage of track overlapping due to accumulation of dislocations and other extended defects was observed. At high fluences (10^{15} ions/cm^2) the hardness saturates at about 3.5 GPa (twofold increase in comparison to a virgin crystal) thus confirming high efficiency of light projectiles in modifications of structure and properties. The depth profiles of hardness indicate on a notable contribution of elastic collision mechanism in the damage production at the end-of-range region. The effects of ion-induced increase of hardness and decrease of dislocation mobility are observed also beyond the ion range and possible mechanisms of such damage are discussed.

Highlights

- The depth profiles of damage in LiF irradiated with ^{3}He and ^{4}He ions were studied.
- High-fluence irradiation creates dislocation-rich structure and induces strong hardening.
- Changes of LiF structure and properties were observed also beyond the ion range.
- Mechanisms of damage beyond the ion range are discussed.

Keywords

LiF crystals, ion-irradiation, ^{3}He and ^{4}He ions, dislocations, nanoindentation, photoluminescence, damage beyond the ion range

1. Introduction

Irradiation with swift ion beams offers ample opportunities to modify under controlled conditions the structure, physical and mechanical properties of functional materials by creation of radiation defects and defect aggregates, extended defects (ion tracks, dislocations, colloids), surface and bulk nanostructures [1-5].

In radiation damage studies, LiF crystals play an important role because of their wide application possibilities (dosimeters, color-center lasers, fluorescent imaging detectors, etc.). LiF serves as a well-studied model material exhibiting high radiation sensitivity and stability of radiation defects at room temperature, and maintains crystallinity under severe irradiation. Besides, LiF is a well-known model material in studies of dislocation structures [6, 7].

Generally, it is widely accepted that swift heavy ions if compared with light ions at likewise fluences are more efficient in production of damage in LiF [1]. However, recent studies have shown that severe irradiation with light ions (^{12}C, ^{14}N) also creates strong structural damage, can cause high concentration of color centers even exceeding that reached by irradiation with high-energy heavy ions [4, 8] and can induce notable strengthening effect despite of large differences in the ion mass, energy, energy loss and track morphology [3, 9].

In this study, damage processes in LiF under irradiation with light projectiles (^{3}He and ^{4}He ions) were investigated. The main attention has been devoted to high dose irradiation at which the overlapping of tracks and formation of complex color centers (F_n), defect nanoclusters and extended defects can occur.

The peculiarity of structural damage in LiF under irradiation with some ions (^{12}C, ^{64}Ni) is the formation of color centers not only in the directly irradiated zone, but also beyond the calculated ion range [10-14]. In order to reveal possible damage effect beyond the range, the damage profiles were studied in an extended depth range.

2. Experimental

Samples were obtained from a single-crystal LiF block grown from a melt in an inert atmosphere (Korth Kristalle, Germany). Thin platelets of 8×8 mm^2 were cleaved along the (100) plane with a thickness of about 1 mm. Samples were irradiated 13.5 MeV ^{3}He ions at a 7 MV Van-de-Graaff accelerator (Frankfurt/M, Germany) and with 5 MeV ^{4}He ions at the UNILAC linear accelerator of GSI (Darmstadt, Germany). All samples were irradiated at room temperature and at the normal incidence of ion beam to (001) crystal face. The fluences (Φ) were 10^{11} – 5×10^{12} ions/cm^2 for ^{3}He ions and 10^{14} and 10^{15} ions/cm^2 for ^{4}He ions. The ion range (R) and energy loss were calculated using SRIM 2013 [15]. The ion range was in all cases less than the sample thickness, i.e., the beam was stopped within the crystals. Average absorbed energy was estimated as $E_{a=} E_{ion}\times\Phi/R$ where E_{ion} is the energy of incoming ions.

The depth profiles of damage were studied using nanoindentation and dislocation mobility methods which are sensitive mainly to dislocations, colloids and other extended defects.

Changes of micro-mechanical properties were characterized by an instrumented nano-indentation unit G200 (Agilent) using a Berkovich diamond tip. Measurements were performed in ambient air at room temperature. The strain rate was $0.05s^{-1}$. For the calculation of hardness and Young's modulus from experimentally obtained loading–unloading curves, the Oliver–Pharr model was used [16]. Profile surfaces suitable for indentation were prepared by cleaving the samples along the direction of ion beam. A basic nanoindentation method was utilized and comparatively small indents (depth 150 nm) were used to ensure a reasonably large number of data points with still acceptable errors. The distance between the irradiated surface and the position of indentation imprints was measured by means of optical microscopy. The Vickers indentation technique was used for the evaluation of dislocation mobility based on the measurements of the arm-length of dislocation rosettes around indentation imprints [17].

The dislocation structure in irradiated LiF samples was revealed by a short-time (~1 s) selective chemical etching in a saturated aqueous $FeCl_3$ solution and a subsequent imaging by atomic force microscope (AFM) in the tapping-mode.

The depth profiles of complex color centers (F_2) were studied by a confocal laser scanning spectromicroscopy. All measurements were performed at room temperature using a confocal microscope with spectrometer Nanofinder-S (SOLAR TII) through a Nikon CF Plan Apo 100× (NA = 0.95) optical objective. A diode pumped solid-state (DPSS) Nd:YAG laser (532 nm, max cw power Pex=150 mW) was used as the excitation source, and the photoluminescence spectra were dispersed by 150 grooves/mm diffraction grating mounted in the 520 mm focal length monochromator. The Hamamatsu R928 photomultiplier tube was employed in confocal-spectral imaging experiments to measure a variation of the intensity of the photoluminescence band maximum at 660 nm across the sample during raster scan.

3. Results and discussion

3.1 Changes of structure and mechanical properties of LiF irradiated with ^{3}He and ^{4}He ions

Fig.1a, b shows the depth profiles of hardness, dislocation mobility and calculated ion energy loss in LiF crystals irradiated with ^{3}He ions at different fluences. At fluences $\Phi \geq 5\times10^{11}$ ions/cm^2 an ion-induced increase of hardness and a decrease of dislocation mobility were observed. The hardening effect increases with the fluence confirming the accumulation of nano-scale defects responsible for the hardening. In the major part of the range the depth profiles of

hardness and dislocation mobility correlate with the depth profiles of electronic energy loss of ions determined by SRIM (Fig.1b). However, the effect of ion-induced hardening occurs also at the depth by few tens of μm exceeding the calculated ion range. The ion-induced effect in dislocation mobility behaves likewise and is observed at even greater depth.

As shown in previous studies, the threshold fluence for ion-induced hardening in LiF corresponds to the initial stage of track overlapping [9] at which the average distance between tracks $d=2(\pi\Phi)^{-1/2}$ approaches the diameter $2r_F$ of the track halo where r_F is the Thevenard radius [4]. For ^{3}He ions, the calculation of the track halo diameter from the optical absorption data gives $2r_F \approx 8.2$ nm. Estimates show that, in order to reach such distance between tracks, the fluence about 5×10^{11} ions/cm^2 is required, which is in good agreement with the observed threshold fluence for detectable hardening (Fig.1a).

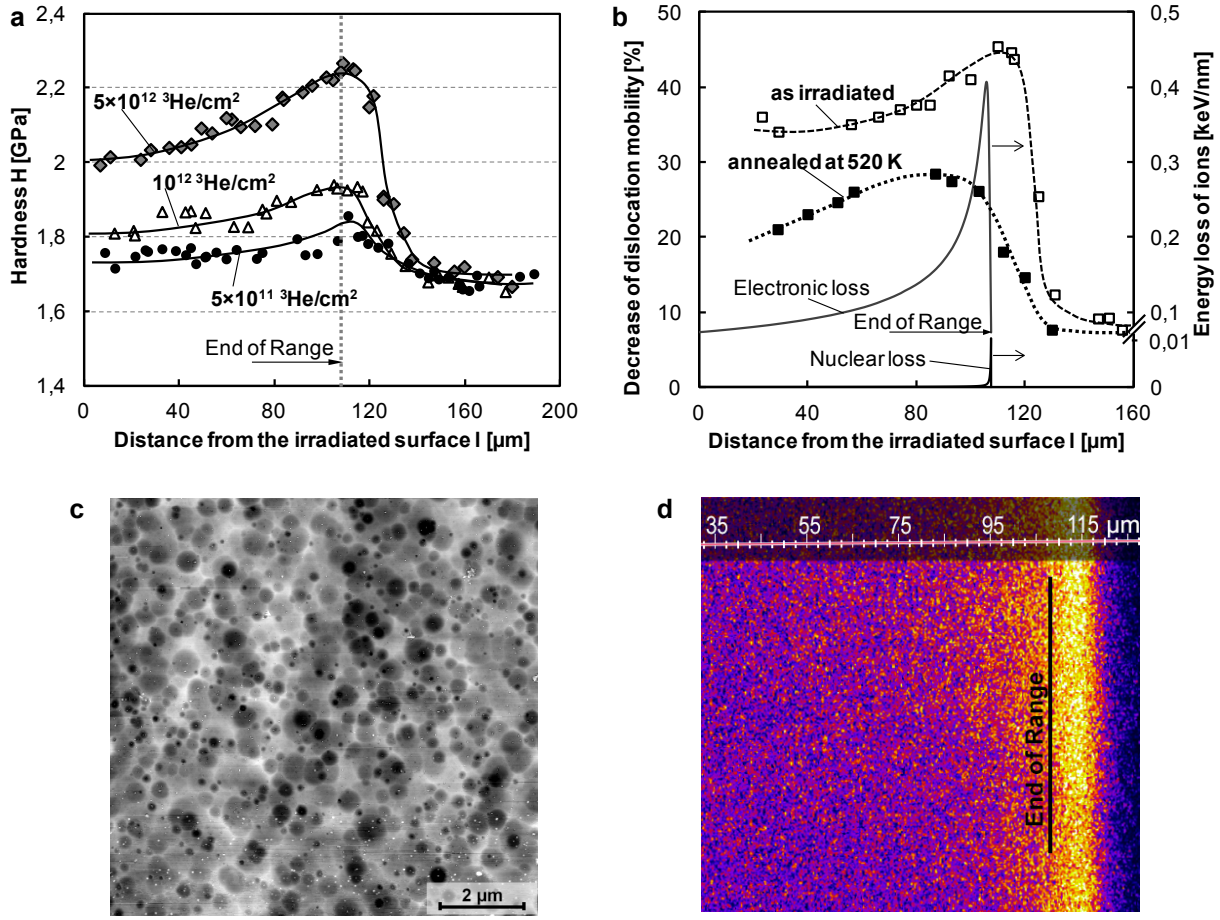

Fig.1. Depth profiles of hardness (a), dislocation mobility (in irradiated at 5×10^{12} ions/cm^2 and annealed at 520 K samples) and calculated electronic and nuclear energy loss of ions (b) in LiF irradiated with 13.5 MeV ^{3}He ions;
AFM image of etched structure in irradiated zone (c) and confocal spectral image of laser-excited photoluminescence for samples irradiated at 5×10^{12} ions/cm^2 (d).

Selective chemical etching [6] on cleaved profile surfaces of irradiated samples reveals etch pits (Fig.1c), which we ascribe to ion-induced dislocations as the main extended defects created in LiF under room-temperature irradiation with swift ions [3, 9]. The rounded shape of etch pits characterizes small dislocation loops or dislocations decorated with radiation defects [7]. Their density at the fluence Φ=5×10^{12} ions/cm^2 reaches ~ 10^9 cm^{-2}.

The peculiarity of the obtained experimental results is the appearance of ion-induced hardening and decrease of dislocation mobility beyond the calculated ion range (Fig.1a, b). With increasing the depth the magnitude of effects gradually decreases, however, the effect in dislocation mobility even at about 300 μm depth still surpasses 10%.

In order to access the saturation stage of damage, the irradiation with ^{4}He ions was performed at higher fluences than in the experiments with ^{3}He ions. The obtained results show a remarkable increase of hardness in LiF irradiated with 5 MeV ^{4}He ions compared with that for a virgin crystal (Fig.2). The hardness of samples inside the irradiated zone shows indications of saturation at Φ=10^{15} ions/cm^2 (dose 166 MGy, average absorbed energy 2.3×10^{24} eV/cm^3). The saturation of hardness is observed in the depth range above 10 μm where its values by a factor of 2.1 exceed the hardness of a virgin crystal (the hardening effect $\Delta H/H_0$= 120%).

The measurements of dislocation mobility show a strong decrease of dislocation arm length around imprints in entire irradiated zone that confirms the presence of strong obstacles for dislocations (Fig.2d). The depth behavior of dislocation mobility is similar to that observed for the depth profiles of hardness (Fig.2a).

Selective chemical etching on irradiated samples reveals numerous square-based etch pits typical for dislocations (Fig.2c and Fig.2e). The density of etch pits at the fluence of 10^{14} ions/cm^2 exceeds 10^{10} cm^{-2}. At the highest irradiation fluence (Φ=10^{15} ions/cm^2) the estimates become impossible due to decrease of etching selectivity and an overlap of etch pits. Etched structures in irradiated zone and outside it are compared in Fig.2c. Generally, outside the irradiated zone the density of etch pits is lower, their respective size is smaller and some of them include few even smaller pits, thus pointing to a possible presence of larger agglomerates.

The effects of hardening and decrease of dislocation mobility in samples irradiated with ^{4}He ions are also observed beyond the ion range. The hardening effect is present at the depth exceeding the calculated ion range by more than 10 μm (Fig.2a) and thus exceeding values of longitudinal straggling of tracks (~0.7 μm) provided by SRIM. The ion-induced effect in dislocation mobility as a more sensitive characteristic is observed in a broader depth range.

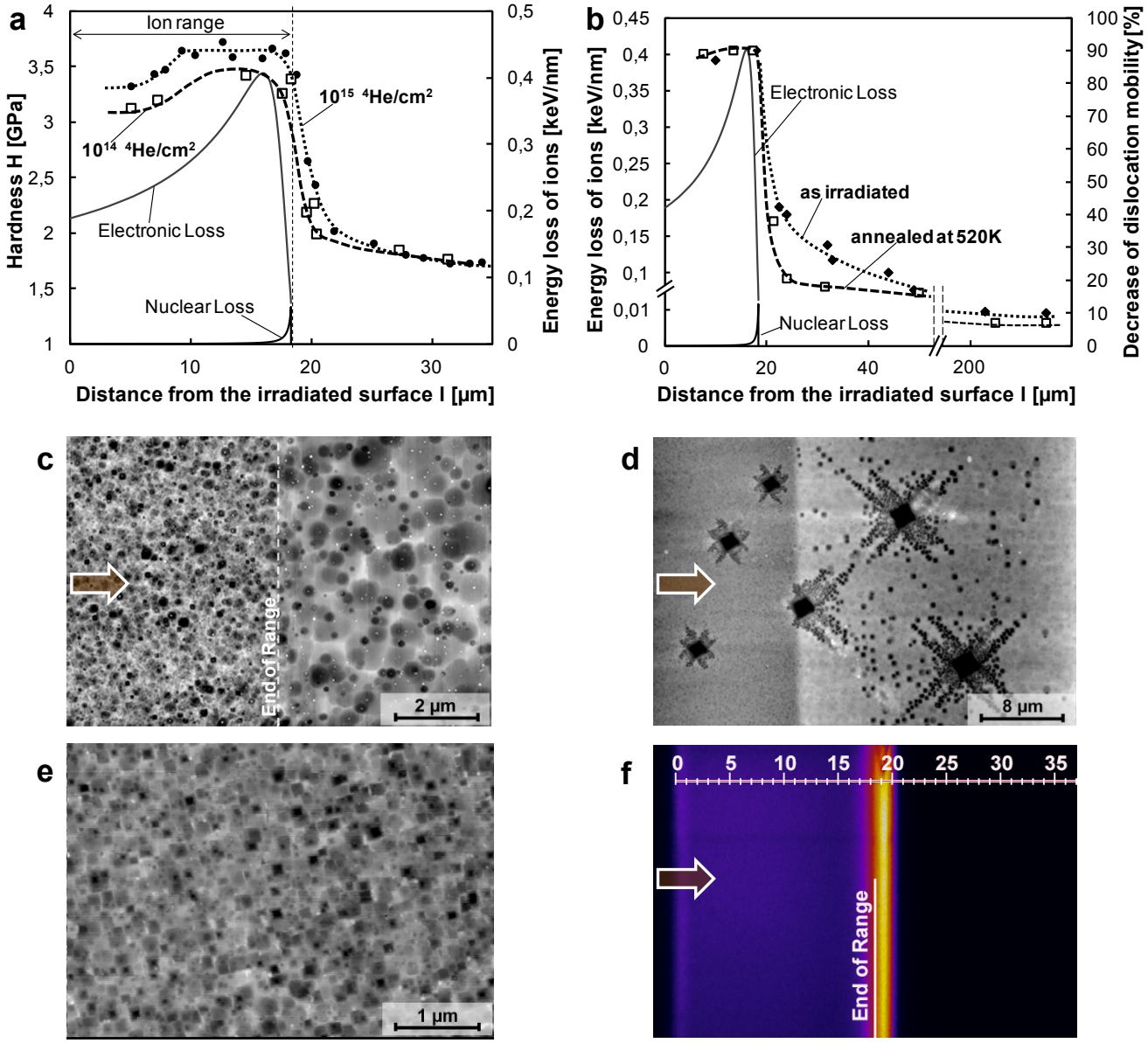

Fig.2. The depth profiles of hardness at different fluences (a) and dislocation mobility (in as-irradiated and annealed at 520 K samples) (b) in LiF irradiated with 5 MeV ^{4}He ions in comparison with the depth behavior of calculated energy loss;
AFM images of etched extended defects in irradiated zone (left) and beyond it (right) in sample irradiated at Φ=10^{15} ions/cm^2 (c);
Dislocation rosettes around indents in irradiated zone (left) and beyond it (right) – (d);
Dislocation structure in irradiated zone at a higher magnification (e) and the confocal spectral image of laser-excited photoluminescence at Φ=10^{14} ions/cm^2 (f). The direction of ion beam is shown by arrows.

3.2. Ion-induced change of optical properties

An additional insight in the evolution of structure of LiF irradiated with ^{3}He and ^{4}He ions is provided by the measurements of optical absorption spectra (Fig.3). Absorption bands at 245 nm (related to *F* centers) and 445 nm (related to aggregate centers, such as F_2 and F_3^+) are observed. In the case of ^{3}He ions, the band of aggregate color centers becomes detectable at the fluence $\Phi \geq 10^{11}$ ions/cm^2 which is close to the threshold fluence for ion-induced hardening. For ^{4}He ions, the used fluences ensure strong overlapping of tracks that leads to aggregation and saturation of primary radiation defects.

In order to visualize the distribution of complex color centers along the ion range, we used confocal microscopy with laser excitation and spectroscopic registration of the F_2 center photoluminescence at 660 nm. The method was effectively used for the investigation of defect distribution along the ion trajectory [19] and provided promising results in visualization of individual tracks of ^{4}He ions [20].

The confocal spectral image of laser-excited photoluminescence of F_2 centers in LiF irradiated with 13.5 MeV ^{3}He ions at $\Phi=5\times10^{12}$ ions/cm^2 is shown in Fig.1d. The brightness of the image on profile surface irradiated to moderate fluences gradually increases along the range and reaches a maximum at the depth of 115 μm (about 15 μm beyond the range). The discrete distribution of bright spots in the obtained image indicates partial overlapping of tracks at the given fluence. In the case of ^{4}He ions (Fig.2f), a uniform coloring is observed, which points to a strong overlap of tracks. The maximum intensity of photoluminescence was observed beyond the range (~2 μm for ^{4}He and ~15 μm for ^{3}He ions).

A comparison of the depth profiles of photoluminescence and hardening shows that the hardening effect occurs in a deeper zone confirming that hardness is determined mainly by non-luminescent extended defects. The difference in depth profiles of photoluminescence of F_2 centers and hardening can be related to luminescence quenching at high absorbed energies (above 10^{24} eV/cm^3) due to the increase of recombination processes at high defect concentration as well as to creation and growth of larger aggregates [19, 21]. The growth of larger aggregates at high fluences can be partly ascribed to interaction of complex color centers with dislocations. The interaction distances between them under conditions of high density of color centers and dislocations (above 10^{10} cm^{-2}) can be achieved despite of the fact that *F* centers are almost immobile at room temperature.

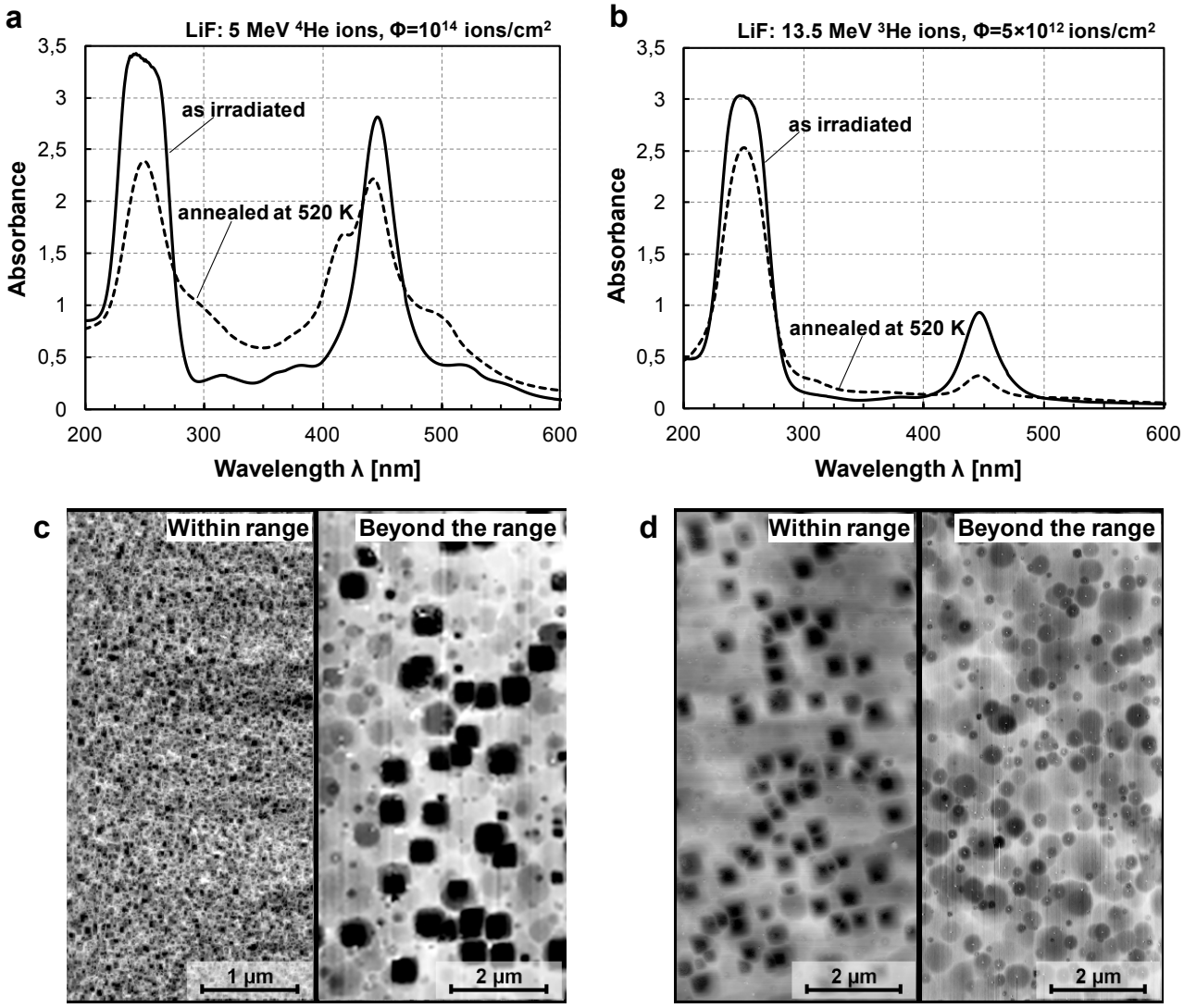

Fig.3. Effect of annealing at 520 K on optical absorption spectra of LiF irradiated with 5 MeV ^{4}He ions (Φ=10^{14} ions/cm^2) (a) and for 13.5 MeV ^{3}He ions (Φ=5×10^{12} ions/cm^2) (b);
AFM images of structure in irradiated zone and beyond it for sample irradiated with ^{4}He ions at Φ=10^{15} ions/cm^2 (c) and for samples LiF irradiated with ^{3}He ions at Φ=5×10^{12} ions/cm^2 (d) after annealing at 550K.

In order to investigate the thermal stability of ion-induced structural defects, the annealing of irradiated samples at moderate temperatures (up to 550 K) during 15 min was performed. After such annealing, the F and F_n center maxima are reduced due to evolution of recombination processes (Fig.3 a,b). Besides, in the heavily irradiated samples (irradiations with ^{4}He ions), annealing leads to a broadening of 445 nm optical absorption band and formation of the band at 415 nm (Fig.3a), indicating accumulation of complex color centers and possible formation of small colloids or their embryos [22]. The structure, created under irradiation with high fluences survives annealing at 550 K (Fig.3c, left). A noteworthy recovery of structure and properties is observed in less damaged areas including zone, irradiated with ^{3}He (Fig.3d,left and Fig,1b) and

beyond–the-range zone for ^{4}He (Fig.3c, right, Fig.1b) where square-based etch pits typical for stable dislocation loops were observed.

3.3. Ion-induced damage and hardening beyond the range

Few decades ago an interesting effect of color center formation in LiF was found at a depth of up to 3 mm beyond the range of swift ^{12}C ions [10]. Recently, color centers far beyond the projected ranges were observed for some heavy ions (8–11 MeV/u ^{64}Ni, ^{102}Ru,^{197}Au, ^{208}Pb, and ^{238}U) in LiF crystals, irradiated with high fluences (10^{12}–10^{13} ions/cm^2) [14].

In the present study, severe damage in LiF including formation of extended defects (presumably dislocation loops) and improvement of hardness was observed also beyond the range of ^{3}He and ^{4}He ions. The strongest modifications appear at the vicinity of irradiated zone (few tens of μm beyond the range), however, detectable effect in dislocation structure manifests in even deeper zone.

Numerous mechanisms of damage beyond the range have been analyzed and the ion channeling and secondary irradiation accompanying nuclear reactions of incident ions with target nuclei are considered as probable reasons for deep coloring of irradiated samples [14]. The observed formation of color centers and strengthening beyond the range of ^{12}C ions in LiF is ascribed to the channeling effect and secondary irradiations from nuclear reactions of incident ions with target nuclei [10, 11, 14].

The channeling effect in our experiments could be excluded because it was found to become negligible at high- fluence irradiations of LiF due to dechanneling of ions on radiation defects and aggregates [23]. Also photoluminescence measurements show no detectable signal from the adjacent out-of-range zone (Fig.1d and Fig. 2f).

In order to assess briefly the impact of secondary particles emitted from nuclear reactions, we have considered all possible non-elastic nuclear reactions with $Z\leq2$ and $A\leq4$ products. Secondary particle flux from the irradiation of ^{6}Li, ^{7}Li, and ^{19}F nuclei with ^{4}He and ^{3}He ions was evaluated using nuclear reaction cross-section data from [24] and nuclear structure data from [25]. When LiF samples are irradiated with 5 MeV ^{4}He ions, the largest cross-sections have: a) inelastic scattering reactions (α,α□); and b) direct nucleon transfer reactions (^{6}Li(α,p)^{9}Be, ^{6}Li(α,d)^{8}Be, ^{7}Li(α,n)^{10}B, ^{7}Li(α,p)^{10}Be, ^{7}Li(α,t)^{8}Be, ^{19}F(α,p)^{22}Ne). Since the energy of scattered ^{4}He ions would be less than that of the primary ion beam, the only secondary nuclear reaction products which could have energy high enough to cause ionization beyond implantation zone are protons, deuterons, tritons and γ-rays. With regard to the proton/^{4}He range ratio in LiF, secondary

proton energy should be greater than 1.3 MeV. At ^{4}He fluence ~10^{15} ions/cm^2, evaluated total secondary particle fluence (without γ, e^- and e^+) is ~1.7×10^{10} cm^{-2}. Estimated secondary particle (protons, deuterons and tritons) fluence beyond the range of ^{4}He ions in LiF is ~10^9 cm^{-2}. The greatest impact on the creation of structural defects would be provided by protons constituting almost 80% of the secondary particle flux.

In the case of LiF samples irradiated with 13.5 MeV ^{3}He ions, the resulting secondary particle flux from nuclear reactions would be higher, than that for irradiation with ^{4}He ions, mostly due to (a)-higher projectile energy; (b)-lower binding energy of ^{3}He nuclei resulting in greater energy yield of corresponding nuclear reactions. At the irradiation fluence ~10^{12} ions/cm^2, evaluated total fluence of secondary particles would be ~8.1×10^8 cm^{-2}, and estimated secondary particle (protons, deuterons and tritons) fluence beyond ^{3}He ion range ~10^8 cm^{-2}. However, defects in LiF crystals beyond the ion range can be created also by other products of nuclear reactions – deuterons and tritons, as well as electrons and positrons from the decay of radioactive reaction products (mostly ^{8}Li,^{17}F, ^{20}F, and in the case of irradiation with ^{4}He ions – ^{22}Ne). The estimates show that the secondary particle flux for ^{3}He and ^{4}He ions could consist mostly of protons. As reported in [26] the irradiation of LiF crystals with protons at fluences above 10^{10} ions/cm^2 creates fluorescent aggregate centers. We can conclude that the flux of secondary particles could be partly responsible for formation of extended defects and decrease of dislocation mobility observed in our experiments. However, the estimated fluence of secondary particles appears to be below the threshold for detectable hardening (~5×10^{11} cm^{-2}, Fig.1a). We can suggest that formation of extended defects and hardening beyond the range is rather a complex phenomenon including contribution of secondary particle flux as well as secondary emissions such as γ- and x-rays, and electrons created in nuclear reactions. Thus, for 100 MeV ^{12}C ions, the β^- emission with 156 keV energy and range in LiF of about 150 μm, which accompanies the creation of ^{14}C isotope in ^{7}Li (^{12}C,^{14}C(β^-) ^{5}Li nuclear reaction, is considered as a possible cause of structural modification and hardening [10, 11].

4. Discussion

A relevant result is comparatively high ion-induced hardening effect created by high-fluence irradiation with light projectiles (Fig.1a and Fig.2a). In order to compare the ion-induced effect for ^{3}He and ^{4}He ions, the dependence of hardening on average absorbed energy for LiF crystals is shown in Fig.4. The results show that at the saturation stage (Φ=10^{15} ions/cm^2, average absorbed energy 2.3×10^{24} eV/cm^3) the obtained hardness values approach those reached by irradiation with MeV and GeV energy heavy ions (Au) [27]. However, for MeV energy ^{3}He, ^{4}He

and Au ions a higher by an order of magnitude average absorbed energy (and correspondingly higher fluence) is required. The observed efficiency of light projectiles in modification of structure and properties is in agreement with previous results for irradiations with MeV energy ^{12}C ions [9]. An advantage of light projectiles is their higher penetration depth compared to heavy ions of the same energy. Thus, the range of 5 MeV ^{4}He ions in LiF is about 19 μm while 5 MeV Au ions can penetrate only to 1.14 μm depth [27]. In the case of heavy ions with GeV energy, spontaneous fracture of heavily irradiated LiF crystals occurs under swelling induced stresses [28].

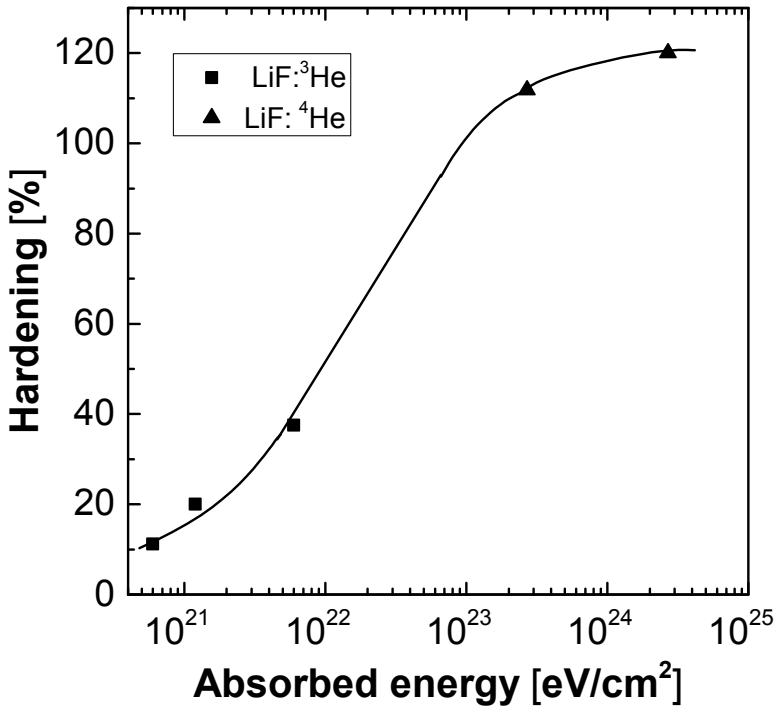

Fig.4. Dependence of the ion-induced hardening on the average absorbed energy for LiF irradiated with ^{3}He and ^{4}He ions.

Prismatic interstitial type dislocation loops are considered as the main extended defects responsible for hardening of LiF irradiated with swift heavy ions at room temperature while single radiation defects are of a minor importance [3, 4].

Embryos of dislocations are found to appear already in individual ion tracks [4] and peculiarities of their growth are considered by Hobbs in [28]. A perfect interstitial dislocation loop in LiF can be formed by the aggregation of equal numbers of anion and cation interstitials as required to maintain the charge neutrality. However it is well established that swift heavy ions in LiF create damage mainly in the anion sublattice by the electronic stopping mechanism, whereas

the cation sublattice remains essentially intact. Also in the present study the electronic energy loss at moderate fluences dominates in a major part of the range (Fig.1a). Hobbs proposed a model in which the formation of dislocations under conditions of electronic stopping occurs when an interstitial di-halide molecule occupies a lattice position and as a result expels an anion and a cation required for dislocation growth. Such reaction becomes possible in the local stress field on edges of existing dislocations and defect aggregates. Therefore, the formation of dislocations under irradiation with light projectiles in the depth range where the electronic stopping is dominating can be explained by the Hobbs' model [29]. However, the contribution of nuclear stopping mechanism which creates the damage in both the anion and cation sub-lattices cannot be neglected, especially in the end-of-range region where the electronic energy loss decreases to low values while nuclear loss displays a maximum. Confirming this, the hardening, which is sensitive to extended defects, displays a maximum for investigated light projectiles in the end-of-range region (Fig.1a and Fig.2a). Due to the contribution of nuclear mechanism in the formation of damage, the zone of hardening at the Bragg maximum becomes extended to a larger depth.

Another peculiarity is the formation of extended defects and notable strengthening beyond the range of ^{3}He and ^{4}He ions in LiF. A related effect – the appearance of color centers in LiF at the surprisingly high depth (up to 3 mm beyond the range) for irradiations with ^{12}C ions was reported in [10, 11] and for some heavy projectiles was observed in [14]. In the present study, stronger structural damage and even the change of mechanical properties under secondary irradiations in the out-of-range zone is observed. The zone of extra hardening extends over tens of μm beyond the calculated range, while the dislocation mobility as a more sensitive method – reveals an affected zone of few hundreds of μm beyond the range. Etching reveals extended defects which presumably could be small dislocation loops; however, the methods used do not allow us to identify them clearly. Moreover, a part of etching figures include few smaller etch pits that could indicate on the presence not only of separate extended defects but also defect agglomerates.

The possible mechanisms of damage beyond the range are still under discussion [14]. We can suggest that formation of extended defects and hardening beyond the range is rather a complex phenomenon including contribution of secondary particle flux as well as secondary emissions such as γ- and x-rays, and electrons created in nuclear reactions. Brief estimates presented in Section 3.3 allow us to suggest that secondary particle flux, in which protons constitute almost 80%, could make a contribution to damage. However, the irradiation with secondary particles solely seems to be insufficient to explain the observed effects in hardening

and a complicity of other products of nuclear reactions including γ-rays, electrons, and others in damage is also suggested.

5. Conclusion

The depth profiles of dislocation structure, dislocation mobility, hardness and photoluminescence of complex color centers in LiF irradiated with 13.5 MeV ^{3}He ions and 5 MeV ^{4}He ions have been studied. Comparison of the results with the depth behavior of calculated energy loss leads to following conclusions:

1. In LiF crystals irradiated with light ions, formation of dislocation-rich structure at fluences corresponding to the stage of track overlapping is observed. This leads to the decrease of dislocation mobility and increase of hardness. The results show that at the saturation stage (fluence up to 10^{15} ions/cm^2, dose 166 MGy, average absorbed energy 2.3×10^{24} eV/cm^3) the obtained hardness values approach those reached by irradiation with MeV and GeV energy heavy ions (Au).
2. The ion-induced effects of structural modification are observed also beyond the ion range and include:
   (a) formation of extended defects at the depth which by few hundreds of μm exceeds the calculated range of ions in LiF,
   (b) the increase of hardness and decrease of dislocation mobility up to depths of few tens of μm beyond the range.

The irradiation with secondary products of nuclear reactions of ions with target nuclei is considered as a likely reason for the beyond-the-range damage.

Acknowledgements

This work has been supported by the Latvian national program IMIS2

References

1. K. Schwartz, C. Trautmann, T. Steckenreiter, O. Geiß, M. Kramer, Damage and track morphology in LiF crystals irradiated with GeV ions, Phys. Rev. B 58 (1998) pp.11232-11240.
2. E.A. Kotomin, A.I. Popov, in: K.E. Sickafus et al. (Eds.), Radiation Effects in Solids, Springer, Amsterdam, 2007, pp. 153–192.

3. R. Zabels, I. Manika, K. Schwartz, J. Maniks, R. Grants, MeV–GeV ion induced dislocation loops in LiF crystals, Nucl. Instr. and Meth. in Phys. Res. B 326 (2014) pp.318–321.
4. K. Schwartz, J. Maniks, I. Manika, A review of colour center and nanostructure creation in LiF under heavy ion irradiation, Phys. Scr. 90 (2015) 094011, pp.1-15.
5. F. Aumayr, S. Facsko, A.S. El-Said, C. Trautmann and M. Schleberger, Single ion induced surface nanostructures: a comparison between slow highly charged and swift heavy ions, J. Phys.: Condens. Matter 23 (2011) 39300, pp.11-23.
6. J. J. Gilman, W. G. Johnston, and G. W. Sears, Dislocation etch pit formation in lithium fluoride, J. Appl. Phys. pp.29 (1958) pp.747-754.
7. J.J.Gilman, W.G. Johnston, Dislocations, point-defect clusters, and cavities in neutron irradiated LiF crystals, J. Appl. Phys., 29, (1958) pp.877-888.
8. A. Dauletbekova, K. Schwartz, M.V. Sorokin, M. Baizhumanov, A. Akilbekov, M. Zdorovets, Energy loss effect on color center creation in LiF crystals under irradiation with ^{12}C, ^{14}N, ^{40}Ar, ^{84}Kr, and ^{130}Xe ions, Nucl. Instr. and Meth. in Phys. Res. B 359 (2015) pp.53–56.
9. R. Zabels, I. Manika, K. Schwartz, J. Maniks, A. Dauletbekova, R. Grants, M. Baihumanov, M. Zdorovets, Formation of dislocations and hardening of LiF under high-dose irradiation with 5-21 MeV ^{12}C ions, Appl.Phys.A 123 (2017) 320, pp.1-8.
10. L.L. Regel, V.R. Regel, S.E. Boriskin, G.G. Knab, A.A. Urusovskaya, L.I. Alekseeva, V.V. Klechkovskaya, Phys. Stat. Sol. (a) 73 (1982) pp.255-266.
11. V.R. Regel, L.I. Alekseeva, A.A. Urusovskaya, G.G. Knab, G.V. Sotserdotova, Radiat. Eff. 82 (1984) pp.157-167.
12. A. Kikuchi, H. Naramoto, K. Ozawa,Y. Kazumata, Damage profiles in alkali halides irradiated with high-energy heavy ions Nucl. Instr. and Meth. in Phys. Res.B 39 (1989) pp.724-727.
13. J. Maniks, I. Manika, R. Zabels, R. Grants, E. Tamanis, K.Schwartz, Nanostructuring and strengthening of LiF crystals by swift heavy ions: AFM, XRD and nanoindentation study, Nucl. Instr. and Meth. in Phys. Res. B 282, (2012) pp.81-84.
14. M.V. Sorokin, K. Schwartz, K.-O. Voss, O. Rosmej A.E. Volkov, R. Neumann, Color centers beyond the swift ion ranges in LiF crystals, Nucl. Instr. and Meth. in Phys. Res.B 285 (2012) pp.24-29.
15. J.F. Ziegler, J.P. Biersack, U. Littmark, The Stopping and Range of Ions in Solids, Pergamon Press, New York, 1985.
16. W.C. Oliver, G.M. Pharr, An improved technique for determining hardness and elastic modulus using load and displacement sensing indentation experiments, J. Mater. Res. **7** (1992) pp.1564-1583.
17. I. Manika, J. Maniks, K. Schwartz, Investigation of heavy ion tracks in LiF crystals by dislocation mobility method, Nucl. Instr. and Meth. in Phys. Res.B 266 (2008) pp.2741–2744.
18. K. Schwartz, A. E. Volkov, M. V. Sorokin, R. Neumann, and C. Trautmann, Effect of irradiation parameters on defect aggregation during thermal annealing of LiF irradiated with swift ions and electrons, Phys. Rev. B 82 (2010) 144116.
19. V.A. Skuratov, N.S. Kirilkin, Yu.S. Kovalev, T.S. Strukova, K. Havanscak, Depth-resolved photo- and ionoluminescence of LiF and Al_2O_3, Nucl. Instr. and Meth. in Phys. Res. B 286 (2012) pp.61-66.
20. P. Bilski, B. Marczewska, Fluorescent detection of single tracks of alpha particles using lithium fluoride crystals, Nucl. Instr. and Meth. in Phys. Res. B 392 (2017) pp.41–45.

21. A.Dauletbekova, K. Schwartz, M.V. Sorokin, A. Russakova, M. Baizhumanov, A. Akilbekov, M. Zdorovets, M. Koloberdin, F center creation and aggregation in LiF crystals irradiated with ^{14}N, ^{40}Ar, and ^{84}Kr ions, Nucl. Instr. and Meth. in Phys. Res. B 326 (2014) pp.311-313.
22. A. Lushchik, Ch. Lushchik, K. Schwartz, E. Vasil'chenko, R. Papaleo, M. Sorokin, A. E. Volkov, R. Neumann, and C. Trautmann, Creation of nanosize defects in LiF crystals under 5- and 10-MeV Au ion irradiation at room temperature, Phys. Rev. B **76** (2007) pp.054114-1 – 054114-11.
23. Hj. Matzke, Channeling of MeV projectiles in diatomic ionic crystals, Phys. Stat.Sol.(a) 8 (1971) pp.99-109.
24. Evaluated Nuclear Data File (ENDF), https://www-nds.iaea.org.
25. ENSDF: Evaluated Nuclear Structure Data, https://www.nndc.bnl.
26. M. Piccinini, F. Ambrosini, A. Ampollini, M. Carpanese, L. Picardi, C. Ronsivalle, F. Bonfigli, S. Libera, M.A. Vincenti, R.M. Montereali, Optical spectroscopy and imaging of colour centres in lithium fluoride crystals and thin films irradiated by 3 MeV proton beams,
Nucl. Instr. and Meth. in Phys. Res. B 326 (2014) pp.72-75.
27. J.Maniks, I. Manika, R. Grants, R. Zabels, K. Schwartz, M. Sorokin, R.M. Papaleo, Nanostructuring and hardening of LiF crystals irradiated with 3–15 MeV Au ions, Appl Phys A 104 (2011) pp.1121–1128.
28. I. Manika, J. Maniks, K. Schwartz, C. Trautmann, M.Toulemonde, Hardening and long-range stress formation in lithium fluoride induced by energetic ions, Nucl. Instr. and Meth. in Phys. Res. B209 (2003) pp.93-97. DOI: 10.1016/S0168-583X(02)02001-3
29. L. W. Hobbs, A. E. Hughes and D. Pooley, A Study of interstitial clusters in irradiated alkali halides using direct electron microscopy, Proc. R. Soc. Lond. A 332 (1973) pp.167-185.

Figure 1

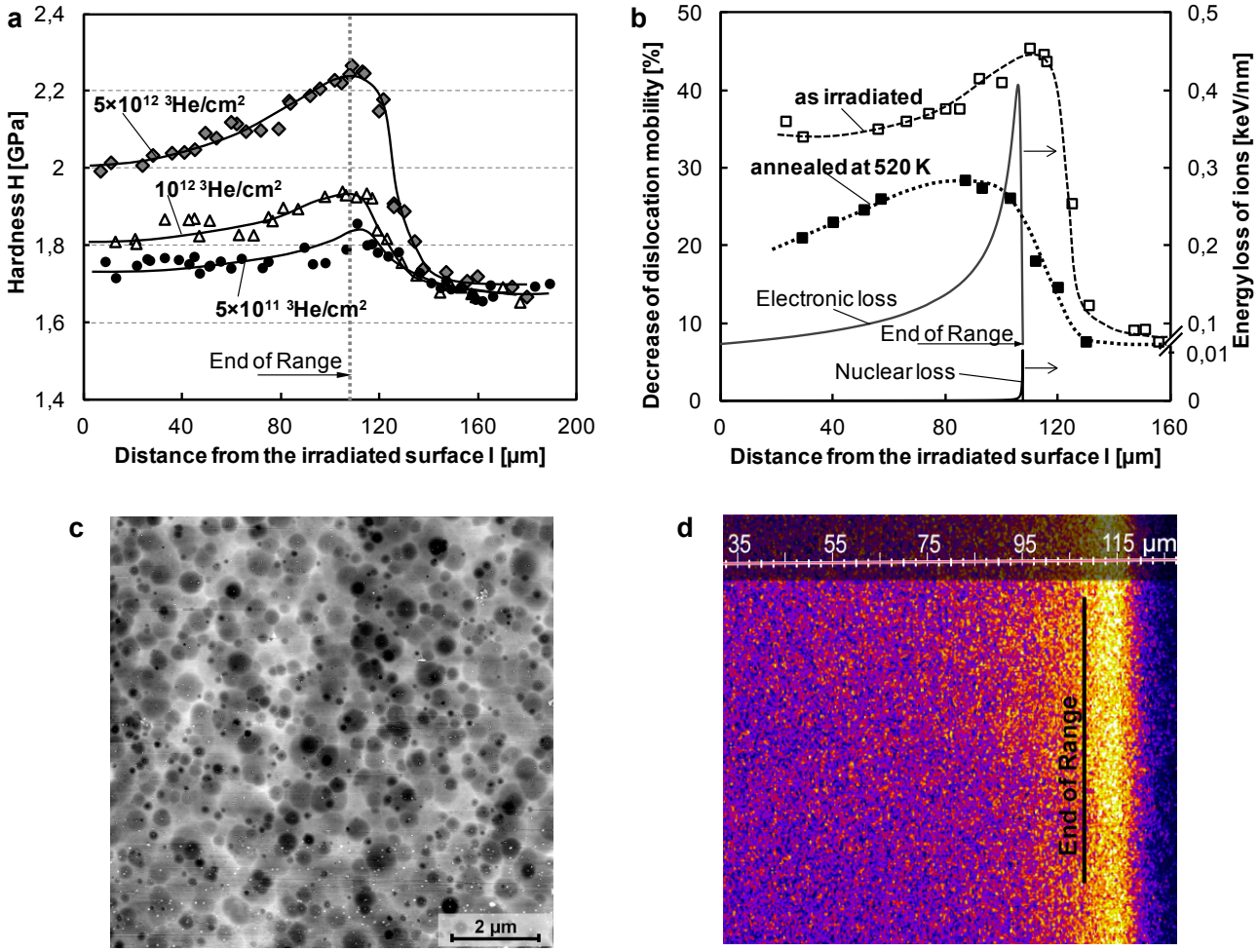
a
Hardness H [GPa]
2,4
2,2
2
1,8
1,6
1,4
5×10¹² ³He/cm²
10¹² ³He/cm²
5×10¹¹ ³He/cm²
End of Range
0
40
80
120
160
200
Distance from the irradiated surface l [μm]
b
Decrease of dislocation mobility [%]
50
40
30
20
10
0
as irradiated
annealed at 520 K
Electronic loss
End of Range
Nuclear loss
0,5
0,4
0,3
0,2
0,1
0,01
0
Energy loss of ions [keV/nm]
0
40
80
120
160
Distance from the irradiated surface l [μm]
c
2 μm
d
35
55
75
95
115 μm
End of Range

Figure 2

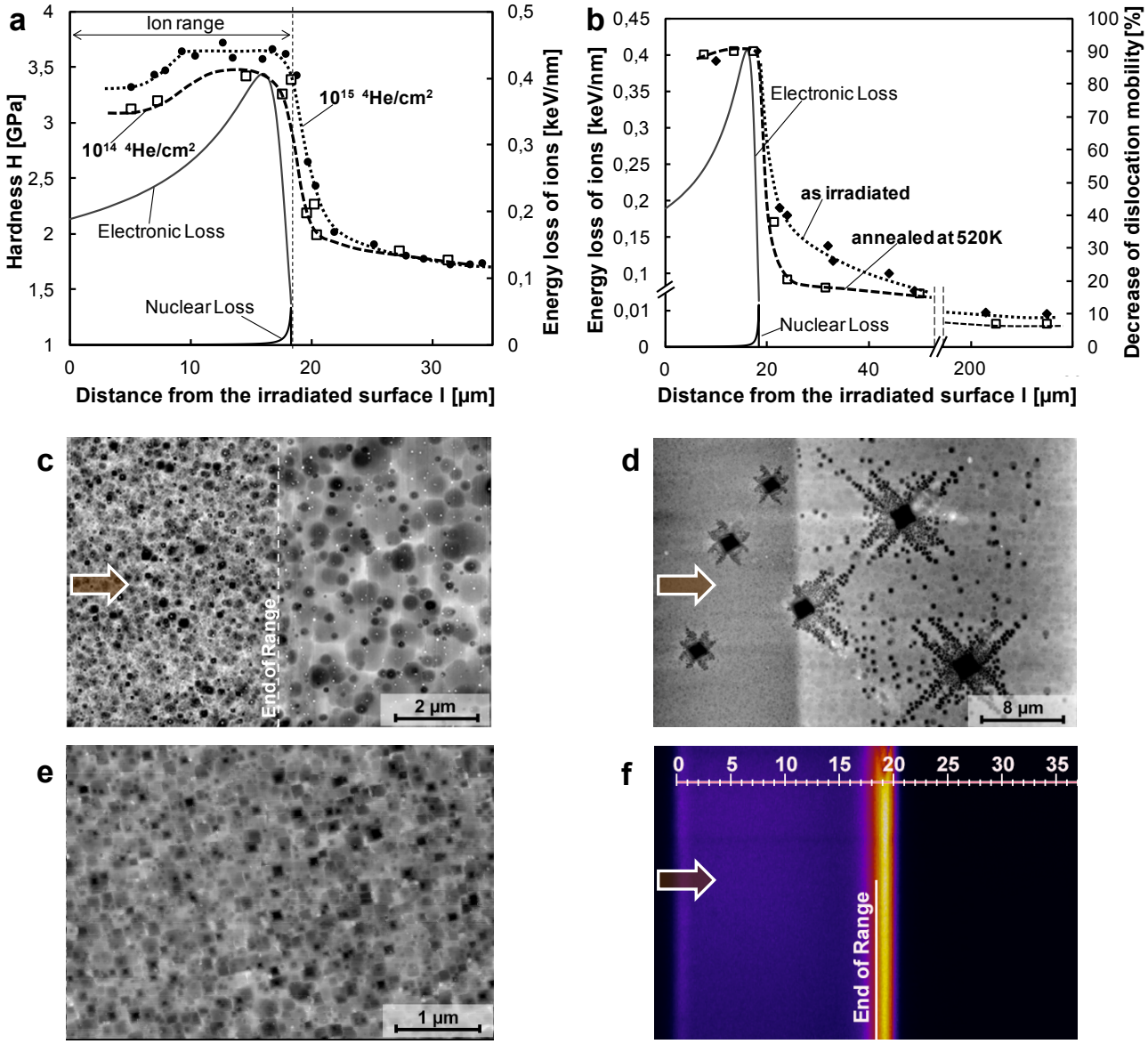
a
Ion range
10^{15} ^{4}He/cm^2
10^{14} ^{4}He/cm^2
Electronic Loss
Nuclear Loss
Hardness H [GPa]
Energy loss of ions [keV/nm]
Distance from the irradiated surface l [μm]
b
Electronic Loss
as irradiated
annealed at 520K
Nuclear Loss
Energy loss of ions [keV/nm]
Decrease of dislocation mobility [%]
Distance from the irradiated surface l [μm]
c
End of Range
2 μm
d
8 μm
e
1 μm
f
End of Range

Figure 3

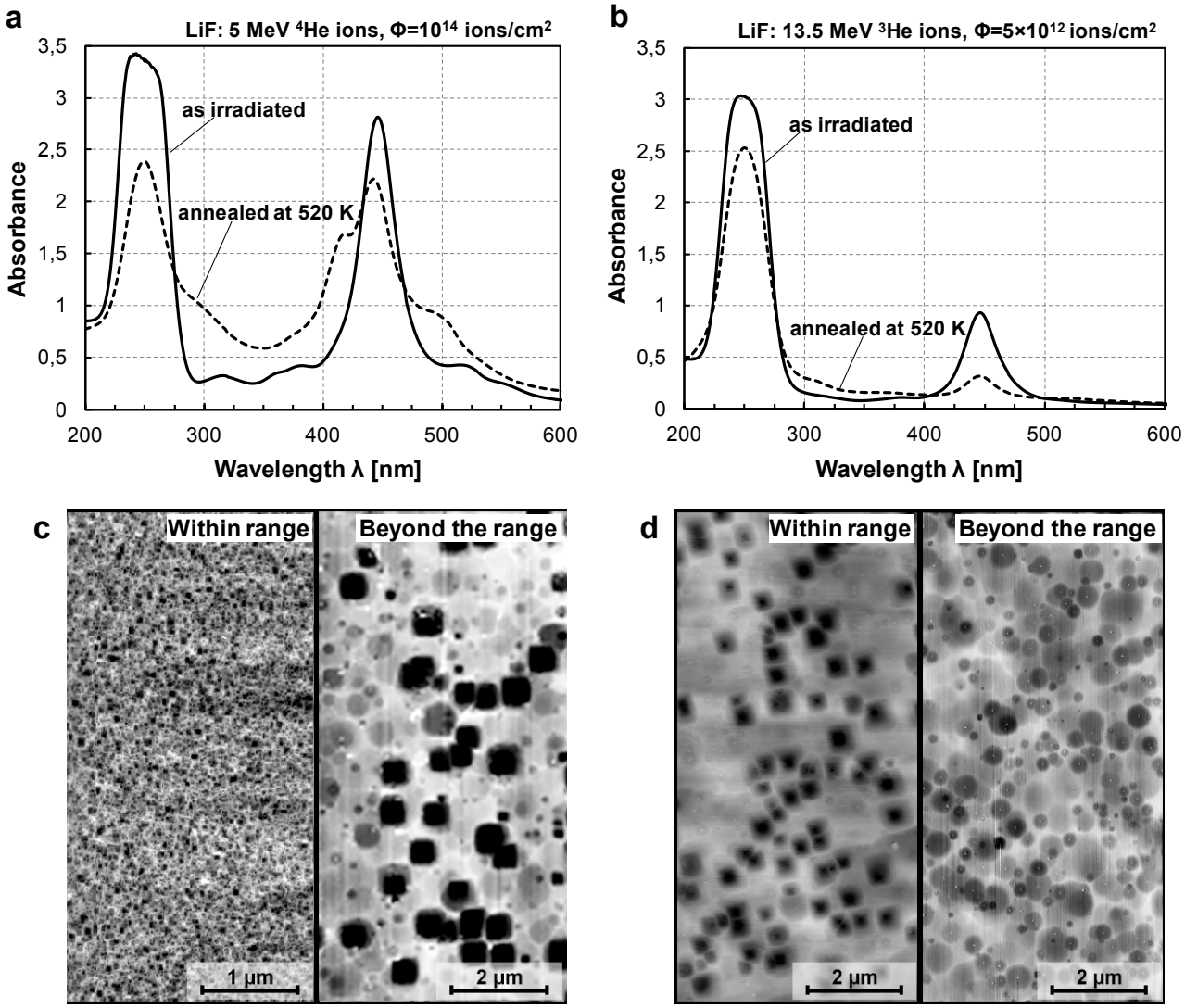
a
LiF: 5 MeV ^{4}He ions, Φ=10^{14} ions/cm^2
as irradiated
annealed at 520 K
Absorbance
Wavelength λ [nm]
b
LiF: 13.5 MeV ^{3}He ions, Φ=5×10^{12} ions/cm^2
as irradiated
annealed at 520 K
Absorbance
Wavelength λ [nm]
c
Within range
Beyond the range
1 μm
2 μm
d
Within range
Beyond the range
2 μm
2 μm

Figure 4

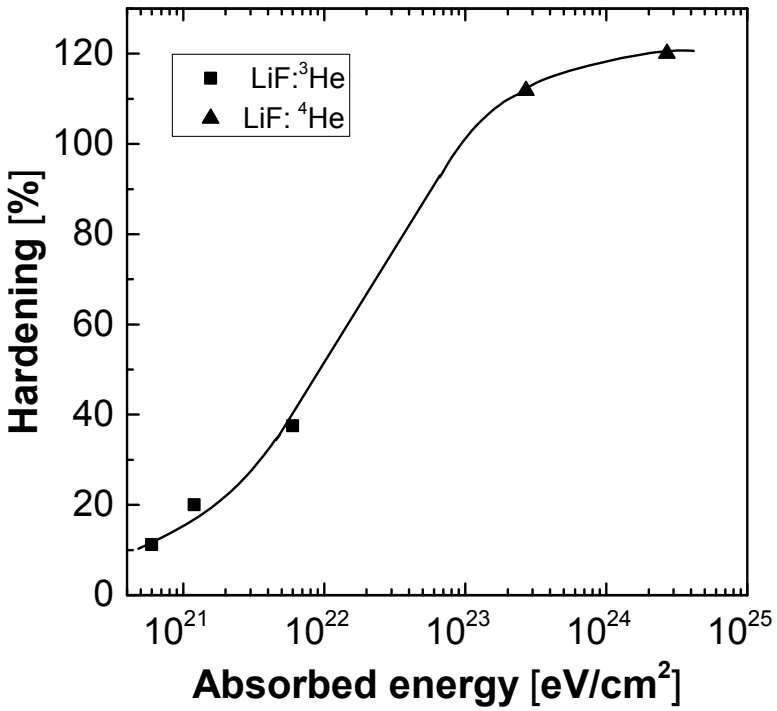

Institute of Solid State Physics, University of Latvia as the Center of Excellence has received funding from the European Union's Horizon 2020 Framework Programme H2020-WIDESPREAD-01-2016-2017-TeamingPhase2 under grant agreement No. 739508, project CAMART²